www.cad-journal.net
Computer-Aided Design AND APPLICATIONS™

Assembly Precision Evaluation of Compressor Using 3D Scan Data

Hayato Asami[1], Yutaka Ohtake[2], Takayuki Nishizawa[3] and Yoji Matsumoto[4]

[1]The University of Tokyo, asami@den.t.u-tokyo.ac.jp
[2]The University of Tokyo, ohtake@den.t.u-tokyo.ac.jp
[3]Daikin Industries, Ltd, takayuki.nishizawa@daikin.co.jp
[4]Daikin Industries, Ltd, youji1.matsumoto@daikin.co.jp

Corresponding author: Yutaka Ohtake, ohtake@den.t.u-tokyo.ac.jp

Abstract. Currently, assembly precision evaluation of machine parts is performed manually. One possible way to automate this process and perform it quickly and stably is to use optical scan data of the parts. However, the accuracy of optical scanners is limited and cannot be used directly for evaluation. Therefore, this study aims to achieve high-precision evaluation by modeling the scan data of cylindrical parts produced by grinding. In experiments on pistons, the radius could be measured with accuracy exceeding the original scanner precision.

Keywords: Assembly Precision Evaluation, 3D Scan, Model fitting
DOI: https://doi.org/10.14733/cadaps.2026.292-301

1 INTRODUCTION

The most important component that determines an air conditioner's performance is the compressor (Fig. 1(a)). Inside the compressor, refrigerant is compressed between the piston and cylinder, and heat is exchanged as the piston rotates. If the gap between the piston and cylinder is too large, the refrigerant leaks, and the pressure does not rise sufficiently; if the gap is too small, the piston does not rotate smoothly, so the compressor assembly's accuracy greatly affects product performance.

Currently, assembly accuracy evaluation is done manually, but a possible way to automate this process and achieve high speed and stability is to measure each component with an optical scanner and evaluate the scan data on a computer. However, the accuracy of optical scanners is limited and cannot simply be used for evaluation.

Therefore, this study aims to evaluate the accuracy of cylindrical parts made by grinding with high accuracy by modeling the scan data (Fig. 1). Using this model, we plan to assemble the parts in software to measure the gap size and calculate the proper attachment positions. There are several methods for modeling cylindrical point clouds, such as meshing, B-spline fitting, and cylinder fitting. Generating a mesh from point clouds is one of the most common approaches. For example, Screened Poisson Surface Reconstruction [3] generates a mesh from point clouds by incorporating positional constraints into the normal Poisson Surface Reconstruction, which helps to prevent excessive smoothing. Boltcheva [2] proposed a parallel and memory-efficient method to generate a mesh

Figure 1: (a) picture of assembly, (b) CAD data, (c) pictures of parts, and (d) scan data (arrows show the radii measured in this study).

using 3D Voronoi diagrams. The advantage of meshing is its high degree of freedom, but it also makes it easier to reflect noise. Since the scan data is noisy at a small scale, meshing is not suitable for this case where high-precision modeling is required. B-spline fitting is also a widely used method. For example, Krishnamurthy [4] proposed a method to fit B-spline surfaces to dense polygon meshes for better representation. Lai [5] adapted B-spline curves for wireframe fairing. While B-spline fitting can construct smooth surfaces, it is still susceptible to noise. Cylinder fitting is a method specifically designed for cylindrical point clouds. Various quadric surface fitting methods, including cylinder fitting, are listed in [1]. Randrup [8] used a cylindrical surface to approximate the shapes of ship surfaces. While cylinder fitting is resistant to noise, it can only construct a perfectly cylindrical model. This is insufficient for this case because the target parts in this study may contain some distortion. Considering the balance between robustness to noise and flexibility, we adopted a method based on linear/parabolic fitting in this study. In addition, to reduce the time required per part, we aim to achieve high accuracy even when multiple parts are scanned at the same time. In the experiment with pistons, the radius could be measured with an accuracy of about 5 microns.

2 METHOD

In this research, the scanned data is processed in the following flow (Fig. 2).

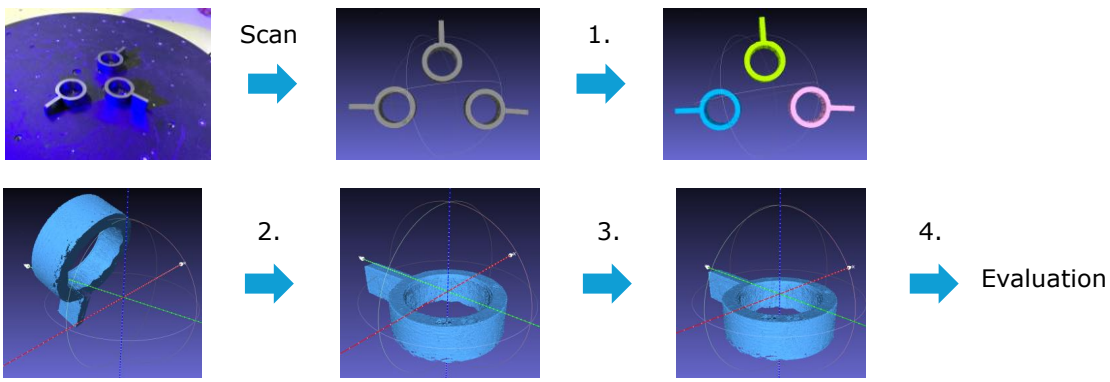

Figure 2: The workflow for processing scan data.

1. Separate each part (in the case of multiple parts scan)
2. Rough alignment to CAD coordinates
3. Precise alignment by linear fitting to a cylindrical surface
4. Surface modeling by linear/parabolic fitting to a cylindrical surface

Each of these is explained in detail below.

2.1 Separate Each Part (in the Case of Multiple Parts Scan)

In the case of multiple scanned parts, the scan data contains multiple parts at the same time, so these parts are first divided into individual parts. In this study, we used a method called the k-means method [6].
The k-means method divides data into a given number of clusters based on distance. Specifically, the process is as follows (Fig. 3).

1. Randomly select k points from the data as cluster centers
2. Assign all points to one of the clusters with the nearest center
3. Find the centroid of each cluster and make it the new cluster center
4. Repeat steps 2-3 until the clusters converge

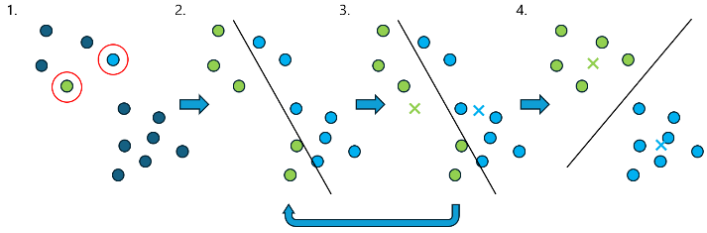

Figure 3: Flow of the k-means method.

2.2 Rough Alignment to CAD Coordinates

The scanned data is described in a camera-related coordinate system. To evaluate the assembly accuracy, a common coordinate system must be used among the parts. The next step of precision alignment requires that the data be roughly aligned. In this study, a method called the RANSAC method [7] was used as a rough alignment method.

In the RANSAC method, we randomly pick a few points to create a model, count how many points (inliers) fit that model, and repeat this process. The model with the most inliers is then chosen to fit the data. Specifically, the process is as follows (Fig. 4).

1. Select two random points from the data, move each point a distance equal to the radius in the normal direction, and connect these new points with a straight line to form the cylinder's axis randomly select two points from the data, and draw a straight line connecting the points that have been moved in the normal direction by the radius from each point, and this is the axis of the cylinder.

2. Count the number of points (inliers) whose distance from the axis is approximately equal to the radius

3. Repeat steps 1-2 and select the axis of the cylinder with the largest number of inliers among them

4. Perform rigid transformation to match the CAD coordinates according to the part using the obtained information on the axis of the cylinder and the position of the centroid, etc.

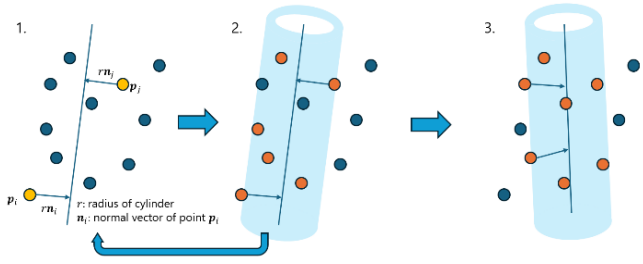

Figure 4: Flow of the RANSAC method.

2.3 Precise Alignment by Linear Fitting to a Cylindrical Surface

Using data roughly aligned by the RANSAC method, the axis of a cylinder is determined and aligned more precisely. In this study, axis updating using straight lines fitted to the cylindrical surface was used as a precise alignment method.

In this method, we first divide the points currently assumed to be on the surface of the cylinder into several regions along the axis of the cylinder. Then, we plot the axial positions z and the distances from the axis r of the points within each region onto the r-z plane and fit a straight line to this plot using the least squares method (Eqn. 2.3.1).

$$r = az + b \tag{2.3.1}$$

$$\text{where } a, b = \arg\min_{a,b} \sum_{i=1}^{n} (az_i + b - r_i)^2$$

These lines are returned to the 3D space as representative lines for each region, and the positions and directions of the axes are updated using these lines, as shown in Fig. 5.

For the position of the axis, we consider a cross-section at the height of the cylinder's center, find the point where the sum of the distances from the intersection of this section and each line is the smallest, and update the axis so that it passes through this point. For the direction of the axis, we find the direction where the sum of the inner products with each line is the largest, and update the axis along this direction. This is repeated multiple times, and when the difference before and after the update is small enough, the update is stopped.

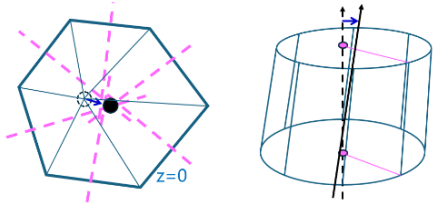

Figure 5: Updating method for the position (left) and the direction (right) of the cylinder axis.

2.4 Surface Modeling by Linear/Parabolic Fitting to a Cylindrical Surface

By fitting straight lines/parabolas to a cylindrical surface of precisely aligned data, a cylindrical surface can be modeled to enable evaluation of assembly precision. Basically, the same operations

are used as those used in the precise alignment process for fitting straight lines. The key points in modeling are tolerance to noise, which is often included in scan data, computation time, and expressiveness of the model. In this study, to find a better modeling method, we tried a total of four different methods, combining two types of norm (L1 norm and L2 norm) used as the distance between the data and the model, and two types of model (linear and parabolic) (Fig. 6.).

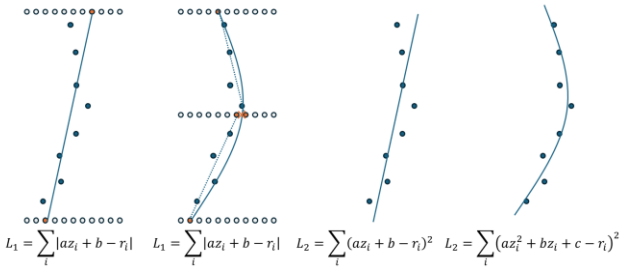

Figure 6: Fitting methods (from left to right: L1-norm-linear fitting (L1-1), L1-norm-pseudo-parabolic fitting (L1-2), L2-norm-linear fitting (L2-1), and L2-norm-parabolic fitting (L2-2))

The L1 norm has the advantage of being robust to noise, while the L2 norm has the advantage of short optimization computation time. In the case of the L1 norm, parabolic fitting requires a much longer optimization computation time than linear fitting, but here, since the computation cannot be completed in a practical time frame, pseudo-parabolic fitting was performed only when the L1 norm was used, as an alternative to regular parabolic fitting. In pseudo-parabola fitting, the data is divided into two parts, upper and lower, within the cylindrical surface, and the three points through which the parabola passes are determined using the results of linear fitting for the upper and lower parts, respectively.

3 EXPERIMENT

The parts to be measured were placed on a turntable and scanned using an optical scanner. Pistons used in air conditioner compressors were used as the measurement target (Fig. 7(a)). Ten pistons were prepared, and all ten were measured individually. An optical scanner ATOS Q from GOM GmbH was used. A lens with a field of view of 170 (350 in the case of multiple parts scan) was used. The turntable was rotated in 10° increments to scan from 36 directions (Fig. 7(b)).

The obtained scan data were modeled using a program we developed, and the radii at each point on the cylindrical surface were evaluated by comparing them with the values measured by a coordinate measuring machine (CMM). The data from the measurement of three parts at once were used only for the parts separation experiment, and the data from the measurement of each part individually were used for the other experiments.

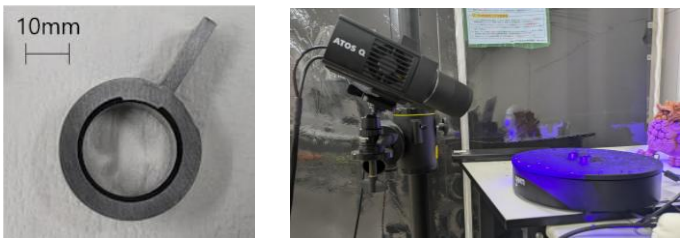

Figure 7: (a) The piston used for measurement and (b) measurement experiment setup.

4 RESULTS AND DISCUSSION

Using the program we created, we performed each of the steps described in Method on the scanned data in turn.
The results of each step are shown below.

1. Separate each part (in the case of multiple parts scan). The data was divided as shown in Fig. 8.
2. Rough alignment to CAD coordinates.
3. Precise alignment by linear fitting to a cylindrical surface. The data was aligned as shown in Fig. 9.
4. Surface modeling by linear/parabolic fitting to a cylindrical surface.

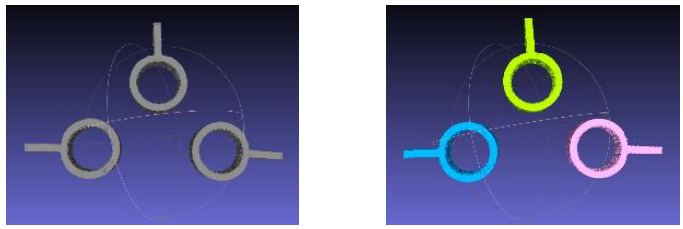

Figure 8: (a) Scan data before separation and (b) scan data after separation.

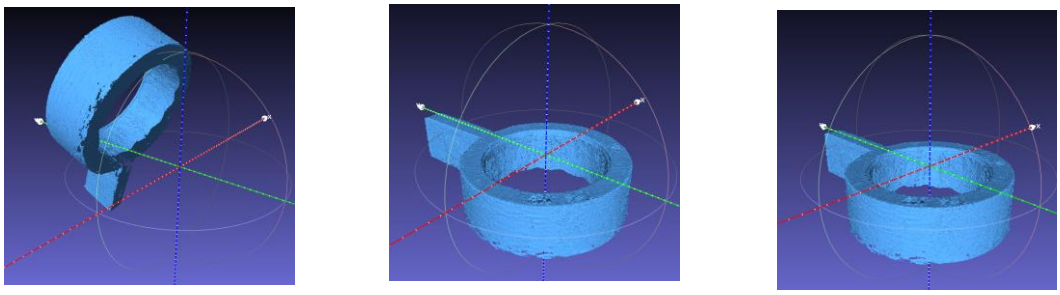

Figure 9: (a) Scan data before alignment, (b) scan data after rough alignment, and (c) scan data after precise alignment.

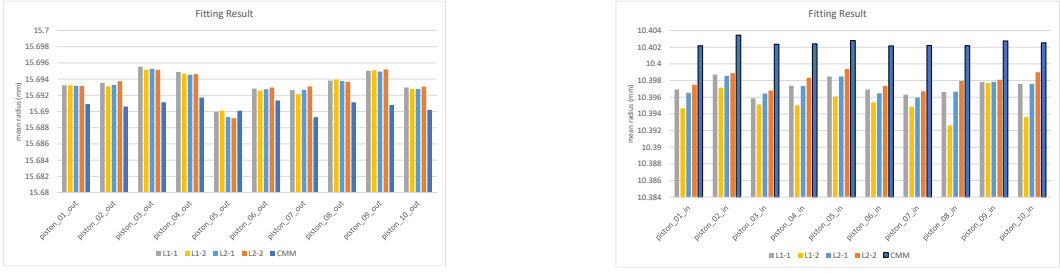

Figure 10: Fitting result of (a) inner radius and (b) outer radius.

The radii of the model were calculated at 45° angles and 1 mm height intervals, and the averages are shown in Fig. 10. The average of the radii at each point measured by CMM is also shown as the correct value.

Figure 11. plots the radius of a piston at a certain angle on the vertical axis and the height along the cylinder axis on the horizontal axis to see how the fitted straight lines and parabolas look.

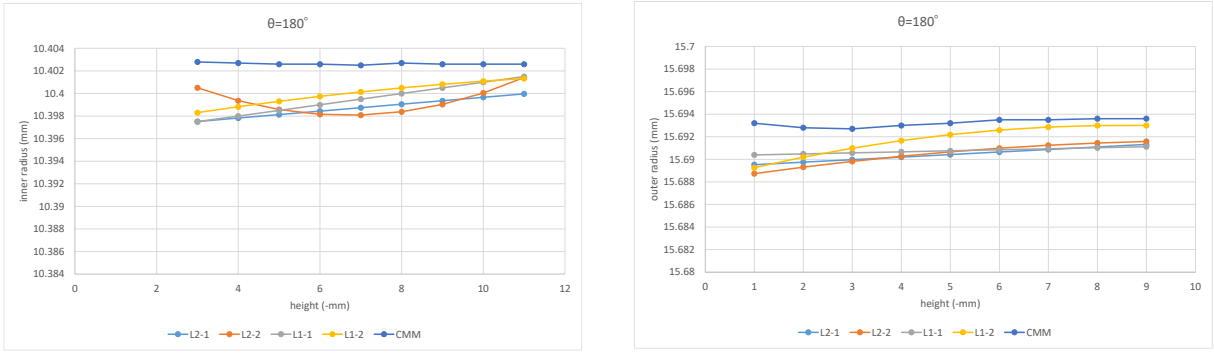

Figure 11: Fitted lines/parabolas of (a) inner radius and (b) outer radius.

Fig. 12 plots the radius of a piston at a height near the center on the vertical axis and the angle along the circumference on the horizontal axis to see how the radius changes with the angle.

Comparing the radius obtained by modeling with the value measured by the CMM, the inner diameter of the scanned data is smaller than the CMM data and the outer diameter is larger. One possible reason for this is the difference in room temperature between measurements with an optical scanner and those with a CMM. In this experiment, the room temperature in the room with the optical scanner was about 5°C higher than that of the room with the CMM, so the piston was more distended during the measurement with the scanner than with the CMM. This point can be addressed by controlling the temperature during the measurement and by making corrections based on the temperature. For example, it is known that the material used for the piston expands by about 1 micron for a change of 5°C. This value can be used for correction. Another possible reason is the effect of the luster of the piston surface. The surface of the piston used has a high gloss and reflects light strongly, which may have caused the object to be misidentified as being closer to the camera than it actually is.

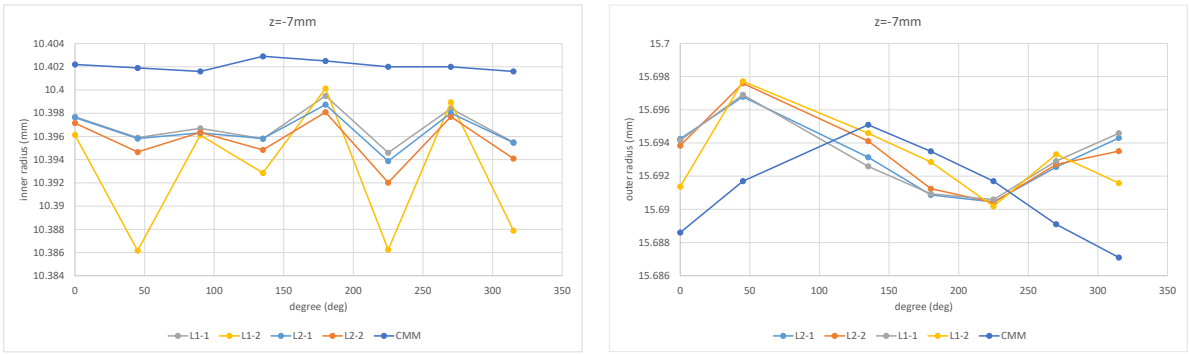

Figure 12: (a) Inner radius and (b) outer radius according to angle.

Looking at the differences between the fitting methods, there were no significant differences in accuracy overall, but in the inner diameter, the L1-norm-pseudo-parabolic fitting showed a larger error in some places. This may be because the lower part of the inner surface is not scanned well. Unlike the other methods, the weights of the entire upper and lower surfaces are equal in the pseudo parabolic fitting, regardless of the density of the points. Therefore, in situations where the density and accuracy of points are high in the upper part of the cylinder and low in the lower part, pseudo-parabolic fitting is more adversely affected by the lower points than the other methods.

In terms of optimization computation time, the L2 norm takes about 0.5 seconds per cylindrical surface, while the L1 norm takes about 12.8 seconds for linear fitting and 16.4 seconds for pseudo parabolic fitting, making the L1 norm 24.0 times and 30.7 times longer than the L2 norm for linear fitting and parabolic fitting, respectively. Since there was no significant difference in accuracy, the L2 norm, which requires less computation time, is preferable in this experiment.

Additionally, although it is still in progress, we tried to evaluate the gap in the assembly. We measured the inner diameter of the cylinder as well as the piston to check the cross-sectional shape and size of the gap between the piston and the cylinder. The front head, crank, piston, and cylinder are assembled as shown in Fig. 13. Fig. 14. shows a graph of the positions of the piston outer surface and the cylinder inner surface relative to the axis of the front head. The results of each fitting on the piston inner surface, piston outer surface, and cylinder inner surface were adjusted so that the radius at the center height matches that of the CMM measurement. For the related values that have not yet been measured, design values were used in the calculation. The distance d_{p} from the axis of the front head to the piston outer surface is determined by $d_{\mathrm{p}} = r_{\mathrm{p,o}} - \max(r_{p,i}) + r_{\mathrm{cr,max}} - r_{\mathrm{f}}$ and the distance d_{cy} from the axis of the front head to the cylinder inner surface is determined by $d_{\mathrm{cy}} = r_{\mathrm{cy}} + \delta$, where $r_{\mathrm{p,o}}$ is the radius of piston outer surface, $r_{\mathrm{p,i}}$ is the radius of piston inner surface, $r_{\mathrm{cr,max}}$ is the maximum distance of the part of the crank, r_{f} is the radius of the hole of front head, r_{cy} is the radius of cylinder inner surface and δ is the offset of cylinder attachment position. From the size of the gaps at each height, which is determined by $d_{\mathrm{cy}} - d_{\mathrm{p}}$, we aim to find the installation position of the cylinder that achieves the desired gap size.

Figure 13: (a) picture and (b) diagram of assembly. (pink: front head, yellow: crank, blue: piston, green: cylinder).

5 CONCLUSIONS AND FUTURE WORK

In this study, we worked on a part of the method to evaluate assembly precision with an accuracy that exceeds the accuracy of the scanner by modeling the scan data of a part made by grinding with a focus on the cylindrical shape of the grinding surface. As a result, we were able to measure the radius of a piston with an accuracy of about 5 microns. In the future, we intend to measure other

parts and evaluate the precision of the gap in the assembled parts based on the scan data for each part.

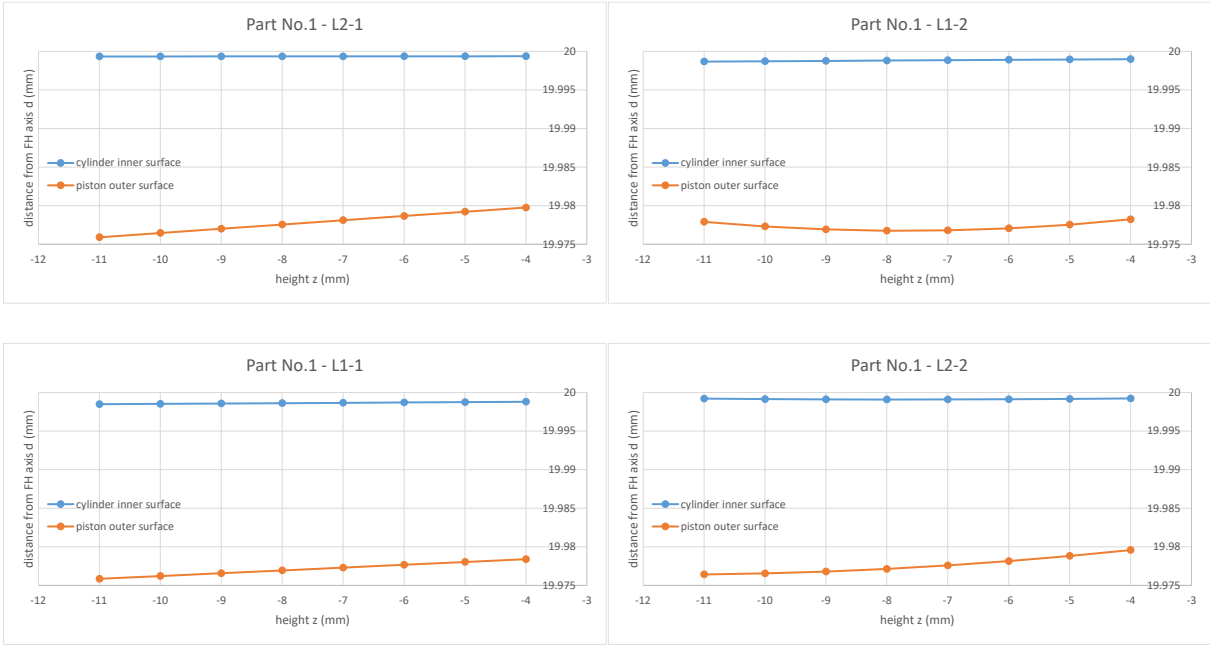

Figure 14: Distance from the axis of the front head to the piston outer surface and the cylinder inner surface in part 1. (a) CMM, (b) L1-1, (c) L1-2, (d) L2-1 and (e) L2-2.

Yutaka Ohtake, https://orcid.org/0000-0002-1368-9172

REFERENCES

[1] Andrews, J.; Sequin, C.: Type-Constrained Direct Fitting of Quadric Surfaces. Computer-Aided Design, 11, 2014, 107-119. https://doi.org/10.1080/16864360.2013.834155

[2] Boltcheva, D.; Lévy, B.: Surface reconstruction by computing restricted Voronoi cells in parallel, Computer-Aided Design, 90, 2017, 123-134. https://doi.org/10.1016/j.cad.2017.05.011

[3] Kazhdan, M.; Hoppe, H.: Screened poisson surface reconstruction, Association for Computing Machinery, 32, 2013. https://doi.org/10.1145/2487228.2487237

[4] Krishnamurthy, V.; Levoy, M.: Fitting smooth surfaces to dense polygon meshes, Proceedings of the 23rd annual conference on Computer graphics and interactive techniques, 1996, 313–324. https://doi.org/10.1145/237170.237270

[5] Lai, Y.; Liu, Y.; Zang, Y.; Hu, S.: Fairing wireframes in industrial surface design, 2008 IEEE International Conference on Shape Modeling and Applications, 2008, 29-35. https://doi.org/10.1109/SMI.2008.4547943

[6] MacQueen, J.: Some methods for classification and analysis of multivariate observations, Proceedings of the fifth Berkeley symposium on mathematical statistics and probability, 1, 1967, 281-297.

[7] Martin, A. F.; Robert, C. B.: Random Sample Consensus: A Paradigm for Model Fitting with Applications to Image Analysis and Automated Cartography, Commun. ACM, 24(6), 1981, 381-395. https://doi.org/10.1145/358669.358692
[8] Randrup, T.: Approximation of surfaces by cylinders, Computer-Aided Design, 30, 1998, 807-812. https://doi.org/10.1016/S0010-4485(98)00038-4